Hot-carrier population inversion in *p*-Ge

Susumu Komiyama and Rüdiger Spies
Institut für Angewandte Physik, Universität Hamburg, Jungiusstrasse 11, 2000 Hamburg 36, Federal Republic of Germany
(Received 22 January 1981)

Hall-effect measurements are performed on *p*-Ge crystals in E up to 3 kV/cm and B up to 5 T at 4.2 K employing a new capacitive method for the detection of the Hall field E_y. At high E levels, there appear in the E_y vs B curves new structures which are interpreted in terms of the population inversion of heavy holes and light holes.

Streaming motion and population inversion of hot electrons as predicted by Maeda and Kurosawa[1] have been established in a series of galvanomagnetic experiments on silver halides.[2–5] Recently Kajita investigated the streaming motion of photoexcited heavy holes in Si.[6] Here we report the observation of population inversion of hot carriers in *p*-Ge in crossed electric and magnetic fields. To our knowledge, this is the first experimental report on the inverted distribution of hot carriers in semiconducting materials.

Hot-carrier phenomena in *p*-Ge have been extensively investigated.[7–9] However, a satisfactory understanding of the phenomena has not been achieved because of the lack of galvanomagnetic measurements in high electric fields at low temperatures. Hence we have extended Hall-effect measurements on relatively pure *p*-Ge crystals to high electric fields up to 3 kV/cm in magnetic fields up to 5 T at 4.2 K. Though the *p*-Ge crystals used here, which have acceptor concentrations of $|N_A - N_D| = 1.1 \times 10^{14}$ and $1.4 \times 10^{14}/\text{cm}^3$, are highly insulating at 4.2 K in low electric fields, they become semiconducting at higher fields due to impact ionization of acceptors.[10] The avalanche breakdown due to impact ionization is observed to take place at $E \sim 5$ V/cm. The hole concentration p as derived from the Hall coefficient is saturated to a value $\sim|N_A - N_D|$ at a field $E > 100$ V/cm. The Hall mobility is 9.0×10^4 and 6.5×10^4 $\text{cm}^2/\text{V sec}$ for the crystals with $|N_A - N_D| = 1.1 \times 10^{14}$ and $1.4 \times 10^{14}/\text{cm}^3$, respectively, both measured at 20 V/cm. Specimens are of a simple rectangular shape ($0.4 \times 3 \times 12$ mm^3) with the crystal orientation shown in Fig. 1. End contacts are prepared by alloying with Au-In (2 at.%).

In order to detect the electric field inside the specimen without causing a distortion of equipotential lines within the specimen, we apply a new capacitive technique instead of the usual contact method with Hall bars. The details of this method will be published elsewhere. As shown in Fig. 1, four small metal plates (0.5×3 mm^2) are put on the specimen with insulating foils (0.1-mm-thick polyethylene) sandwiched between the plates and the specimen. In pulsed measurements the potential at the specimen surface under the metal plates can be detected through the capacitance C formed between the metal plates and the specimen. Absolute values of E_x and E_y can be calculated from detected signals by taking into account the value C and the electrode geometry. The specimen is immersed in liquid helium. Short voltage pulses of 20-nsec duration are applied to the specimen at a repetition rate of 30 Hz by use of the discharge of a 50-Ω coaxial cable. With such short pulses sample heating and the minority carrier injection are avoided. The current through the specimen,

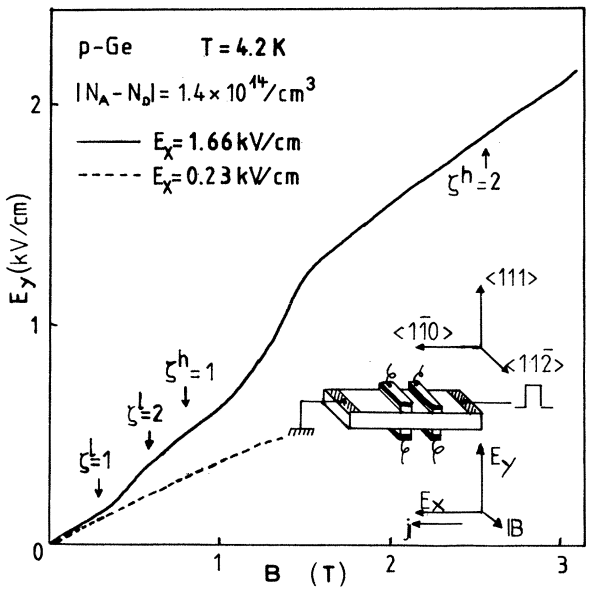

FIG. 1. Recorder traces of E_y vs B at E_x below and above 400 V/cm. Similar curves with the symmetry, $-E_y$, are obtained upon the reversal of the direction of B. Arrows indicate the magnetic fields where Eq. (2) is satisfied. The configuration of the sample with capacitive electrodes is also shown.

j, is measured with a series resistance of 1 Ω.

The drift velocity v_d, as calculated from j and $p = |N_A - N_D|$, is saturated to a value $(9.3 \pm 0.2) \times 10^6$ cm/sec at high electric fields $E_x > 400$ V/cm. The saturated value is close to the half of $V_{OP}^h = 1.9 \times 10^7$ cm/sec, where $V_{OP}^{h,l}$ are defined by the relation

$$\frac{1}{2} m_{h,l}^* (V_{OP}^{h,l})^2 \equiv \hbar\omega_{OP} \ , \qquad (1)$$

where $\hbar\omega_{OP} = 37$ meV is the optical phonon energy and $m_h^* = 0.35 m_0$ and $m_l^* = 0.043 m_0$ are the heavy- and light-hole effective masses, respectively. This fact strongly indicates the streaming motion of heavy holes.[7,9] Further, the collision time $\bar{\tau}_{imp}$ due to ionized acceptor scattering averaged over energies $\epsilon < \hbar\omega_{OP}$ is estimated to be about 12 and 9 psec for the two crystals, respectively. For $E > 400$ V/cm, those $\bar{\tau}_{imp}$ are longer than the traveling time, $T_{OP}^h \equiv (2 m_h^* \hbar\omega_{OP})^{1/2} (eE)^{-1}$, for heavy holes initially at $\epsilon = 0$ to reach $\epsilon = \hbar\omega_{OP}$. ($T_{OP}^h$ at 400 V/cm is ~9 psec.) Thus streaming motion is expected to occur at $E > 400$ V/cm. We also expect light holes, which have a density ~2% of that of heavy holes,[9] to perform streaming motion at even lower fields. However, their small contribution to j cannot be discerned.

To ascertain the streaming motion further and seek the occurrence of population inversion, we have measured the fields E_x and E_y as a function of B at various levels of applied voltage. At any voltage, the field E_x is observed to be almost independent of B, as readily expected from the sample geometry. At low E_x levels ($E_x < 400$ V/cm), the E_y vs B curve is smooth as show in Fig. 1. At low B (e.g., 0.05 T), E_y increases sublinearly with increasing E_x until it is saturated to a constant value above $E_x \sim 300$ V/cm. This reflects the rapid decrease in the mobility of carriers with E_x. At higher E_x levels ($E_x > 400$ V/cm) where the carriers are expected to be streaming, there emerge distinct structures in the E_y vs B curve as shown in Fig. 1. Arrows in Fig. 1 indicate the magnetic fields where the relation

$$\zeta^{l,h} \equiv V_{OP}^{l,h} / V_y = 1 \text{ or } 2 \qquad (2)$$

is satisfied. Here V_y is defined by $V_y \equiv (E_x^2 + E_y^2)^{1/2}/B$ and $V_{OP}^l = 5.5 \times 10^7$ cm/sec is obtained from Eq. (1). E_y increases linearly with increasing B in the small B range $\zeta^l < 1$. Then follows a rapid increase of E_y in the range of B, $1 < \zeta^l < 2$, until the rapid increase is quenched at $\zeta^l \sim 2$. A second steep rise in E_y occurs at B above $\zeta^h \sim 1$, but it levels off before $\zeta^h = 2$ is reached. Similar structures are observed in all the E_y vs B traces taken on the two crystals at different levels of E_x above 400 V/cm. In Fig. 2 the magnetic fields above which E_y rises steeply are plotted as a function of $E \equiv (E_x^2 + E_y^2)^{1/2}$. Solid lines in the figure are drawn according to Eq. (2). The relatively good agreement of the observed values with

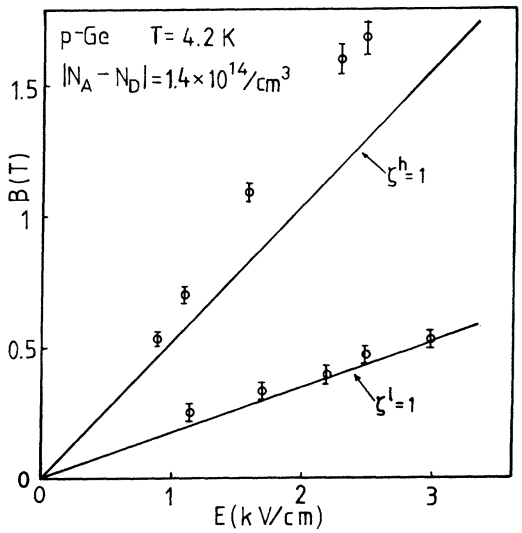

FIG. 2. Magnetic field positions B above which E_y increases abruptly, as a function of $E \equiv (E_x^2 + E_y^2)^{1/2}$. Solid lines are drawn according to Eq. (2).

the theoretically expected values assures the occurrence of population inversion as will be discussed below.

In contrast to Si,[6] the heavy-hole band in Ge (Ref. 11) is nearly parabolic and the mass anisotropy is not very significant in the range $\epsilon < \hbar\omega_{OP}$. Therefore we can consider the phenomena using a scheme developed in Ref. 5 for parabolic and isotropic bands. The trajectory of an ideally streaming carrier in velocity space is shown in Fig. 3 for the cases (a) $\zeta < 1$, (b) $1 < \zeta < 2$, and (c) $2 < \zeta$. Here ζ denotes either ζ^l or ζ^h. In the weak B range $\zeta^l < 1$, both the light and heavy holes perform the circular streaming motion [Fig. 3(a)]. The measured values of E_y in the range $\zeta^l < 1$ can be quantitatively explained from the Hall angle $\tan\theta \equiv E_y/E_x$ determined by the streaming motion[12] of heavy and light holes within an accuracy of 25%. In the higher B range $\zeta^l > 1$, the simple picture of streaming motion is insufficient to explain the observed features in the E_y vs B curves. In the range $1 < \zeta^l < 2$, the center of the circular orbit of the streaming motion, the point C (with coordinates $v_\parallel = 0$ and $v_\perp = -V_y$, where $\vec{v}_\parallel \| \vec{E}$ and $\vec{v}_\perp \perp \vec{E}, \vec{B}$), enters the surface $|\vec{v}| = V_{OP}^l$. There consequently appears within the surface $|\vec{v}| = V_{OP}^l$ an area K^l where the collision time of carriers is long.[1] The area K is shown in Fig. 3(b) with a hatched region. A certain amount of holes are able to accumulate in this area via the following mechanism. A streaming heavy hole may occasionally over run the energy $\hbar\omega_{OP}$ to reach a state $\hbar\omega_{OP} + \Delta\epsilon$ and then jump into the area K^l in the light-hole band after the optical-phonon emission.[13] The probability of this process may be low because of the small density of states in the

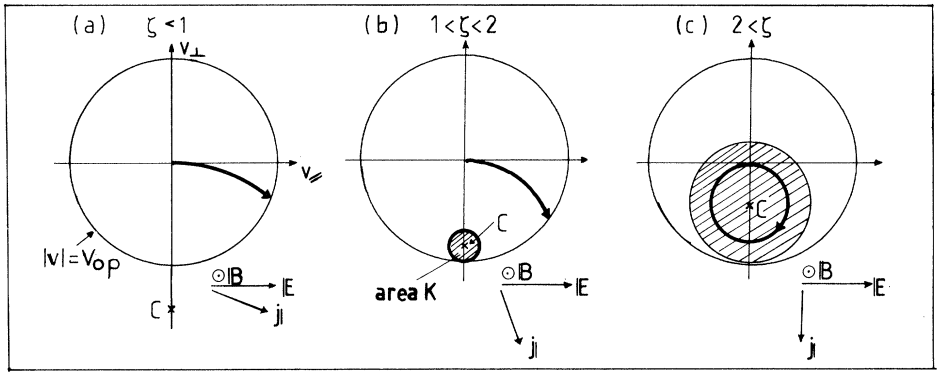

FIG. 3. Trajectory of an ideally streaming carrier in the $v_Z = 0$ plane where $\vec{v}_Z \| \vec{B}$. ζ and V_{OP} denote $\zeta^{l,h}$ and $V_{OP}^{l,h}$ depending on the carrier in question. The point C represents the center of cyclotron orbits in the crossed fields; $C(v_\parallel = 0, v_\perp = -V_y)$. (a) The point C is located outside the circle $|\vec{v}| = V_{OP}$ when $\zeta < 1$. (b) The point C is within the circle and there appears a new area K in addition to the trajectory for streaming motion when $1 < \zeta < 2$. (c) The trajectory for streaming motion disappears when $\zeta > 2$.

light-hole band. Nevertheless, the accumulation is probable since the heavy hole repeats the phonon emission very frequently ($T_{OP}^{h\,-1}$), whereas the scattering event in the area K^l is rare (τ_{imp}^{-1}). The accumulation of light holes in K^l gives rise to an abrupt increase in the Hall angle. This explains the rapid increase in E_y above $\zeta^l = 1$. Above $\zeta^l = 2$, the mean drift velocity of those light holes in K^l, $|\vec{v}| = V_y$, decreases with ζ^l and the contribution of these light holes to the Hall angle decreases. As B increases further to cover the range $\zeta^h > 1$, the point C even enters the surface $|\vec{v}| = V_{OP}^h$ and a similar region ζ^h appears for heavy holes. The carrier accumulation into K^h takes place via a similar mechanism, as above. The accumulation here may be even stronger than that into K^l because of the higher state density in the heavy-hole band. This again results in an abrupt increase in the Hall angle and thus explains the steep rise in the E_y vs B curve above $\zeta^h \sim 1$. A small discrepancy between the observed positions of the steep rise and the theoretically expected positions $\zeta^h = 1$ (Fig. 2) may be attributed to an anisotropy of the heavy-hole band. From the quench of the rapid increase in E_y at $\zeta^h < 2$, one may conclude that almost all the heavy holes already transfer into K^h before $\zeta^h = 2$ is reached. At the still higher ζ^h the streaming motion becomes insignificant and even impossible when ζ^h exceeds 2 [Fig. 3(c)]. At such high ζ^h, the Hall angle[14] is determined by the residual impurity scattering of carriers in K^h, the probability of which is, most simply, independent of B. This qualitatively explains the fact that E_y is nearly proportional to B in the range $\zeta^h \gtrsim 2$. Thus all the observed features of E_y can be well interpreted in terms of the combination of streaming motion of carriers and carrier accumulation into K^l and K^h in velocity space.

The most interesting feature of the phenomena observed here is that the carrier distribution into K^l and K^h manifests a population inversion. Maeda and Kurosawa first predicted such a population inversion for heavy holes in p-Ge on the basis of a Monte Carlo calculation.[1] We conclude here that the population inversion of both the light and heavy holes has been detected for the first time in the present experiment.

ACKNOWLEDGMENT

We want to thank Jörg P. Kotthaus for his encouragement of this work and the critical reading of the manuscript.

[1]H. Maeda and T. Kurosawa, in *Proceedings of the Eleventh International Conference on the Physics of Semiconductors, Warsaw, 1972* (Elsevier, New York, 1972), p. 602.
[2]S. Komiyama, T. Masumi, and K. Kajita, in *Proceedings of the Thirteenth International Conference on the Physics of Semiconductors, Roma, 1976* (Tipografia Marves, Roma, 1976), p. 1222.
[3]S. Komiyama, T. Masumi, and K. Kajita, Phys. Rev. Lett. 42, 600 (1979).
[4]S. Komiyama, T. Masumi, and K. Kajita, Solid State Commun. 31, 447 (1979).
[5]S. Komiyama, T. Masumi, and K. Kajita, Phys. Rev. B 20, 5192 (1979).
[6]K. Kajita, Solid State Commun. 31, 573 (1979).
[7]W. E. Pinson and R. Bray, Phys. Rev. 136, A1449 (1964).
[8]L. Reggiani, C. Canali, F. Nava, and G. Ottaviani, Phys. Rev. B 16, 2781 (1977).
[9]T. Kurosawa and H. Maeda, J. Phys. Soc. Jpn. 31, 668 (1971).

[10]N. Sclar and E. Burstein, J. Phys. Chem. Solids 2, 1 (1957).
[11]E. O. Kane, J. Phys. Chem. Solids 1, 82 (1956).
[12]See Eq. (19) in Ref. 5. Although Eq. (19) is deduced for the transient condition, the quantity $\tan\theta \equiv v_y/v_x$ is identical to $\tan\theta \equiv E_y/E_x$ in the steady-state condition within the approximation of the isotropic band. The measured values of E_y in the range $\zeta^l < 1$ are smaller than those calculated from Eq. (19) by ~25%, presumably due to the anisotropy of the heavy-hole band.
[13]Streaming light holes may also supply carriers into K^l. This process, however, is not significant because of the smaller concentration of the light holes.
[14]If the carriers are free from any scattering mechanisms, $\tan\theta$ is infinite in the range $\zeta > 2$, as seen from Fig. 3(c).